ADVANCED MATERIALS INTERFACES
www.advmatinterfaces.de

A Printing-Centric Approach to the Electrostatic Modification of Polymer/Clay Composites for Use in 3D Direct-Ink Writing

Brittany M. Rauzan, Sean E. Lehman, Joselle M. McCracken, Jonghun Lee, Xiao-Min Lin, Alec Sandy, Suresh Narayanan, Simon A. Rogers, and Ralph G. Nuzzo**

Polymer/clay composite inks are exceptionally useful materials for fabrication processes based on 3D direct-ink writing, however, there remains an insufficient understanding of how their physiochemical dynamics impact printability. Using a model system, *N*-isopropylacrylamide/Laponite, the electrostatic interactions between Laponite platelets are modified to tune critical rheological properties in order to improve printability. Rheological measurements and X-ray scattering experiments are carried out to monitor the nano/micro-structural dynamics and complex physicochemical interactions of Laponite as it impacts complex modulus in the linear region, flow behavior, thixotropy, and yield stress of the composite ink. Modification of the electrostatic interactions between platelets reduces the yield stress of the material, while maintaining a complex microstructure that allows for sufficient recovery times upon removal of stress to form stable, and thus printable, filaments. A printing-centric approach is established based on a fundamental understanding of electrostatic inter-particle interactions, harnessing the innate microstructure of Laponite in 3D direct-ink writing of composites.

The modification of yield-stress fluids for use in direct-ink writing (DIW), a powerful method of 3D printing, is explored with a focus on an exemplary polymer/clay composite ink of current interest for use in the fabrication of soft-material actuators[1] and sensors.[2] While intensively studied, there remains an incomplete understanding of how microscopic features of the physiochemical dynamics of these composites impact their printability. We demonstrate using a model system, *N*-isopropylacrylamide/Laponite (NIPAM/Lap), that modification of the electrostatic interactions between the Lap platelets[3] can be used to tune critical rheological properties to improve printability. Rheological and X-ray scattering measurements were carried out to characterize the nano-/microstructural dynamics of the ink materials and the impacts that electrostatic modifications have on their rheology, including the steady-state flow properties, thixotropy, and yield stress. Means to modify the clay platelet interactions are described that serve to reduce the yield stress of the ink, while affording sufficiently rapid recovery time postextrusion to form stable filaments. A qualitative model of interparticle interactions is described that accounts well for the improvements seen in the DIW of the Lap composites.

DIW is a facile additive manufacturing method, one with features and an enabled range of materials that are of increasing interest for use in the fabrication of soft-material devices including sensors and actuators embedding such functional materials as polymers,[4] hydrogels,[5] and nanocomposites.[6] The composition of the soft-material components present in such devices is critical due to the fine balance that typically exists between the final application-specific properties required of the soft-material components[7] and those necessary for microextrusion of a material with high shape retention.[4] Ideal materials affording useful and broadly tunable capacities for the modification of properties include polymer/clay composites, systems that can provide high shape retention fidelity and capabilities for functional/responsive physicochemical behaviors for use with numerous stimuli: temperature,[8] pH,[9] salt concentration,[10] and electrical fields[11] as notable exemplars. An exemplary clay-based nanocomposite that has attracted increasing interest is NIPAM/Lap, a 3D printable stimuli responsive material. In devices constructed using this material, DIW provides a means that can be used to control the anisotropy of its actuatable responses. These effects can be amplified with appropriate compositional modifications, such as in NIPAM/Lap/cellulose

Dr. B. M. Rauzan, Dr. S. E. Lehman, Dr. J. M. McCracken, Prof. R. G. Nuzzo
Department of Chemistry
University of Illinois at Urbana-Champaign
600 S. Matthews Avenue, Urbana, IL 61801, USA
E-mail: r-nuzzo@illinois.edu
Dr. J. Lee, Dr. A. Sandy, Dr. S. Narayanan
X-ray Science Division
Advanced Photon Source
Argonne National Laboratory
9700 South Cass Avenue, Argonne, IL 60439, USA
Dr. X.-M. Lin
Center for Nanoscale Materials
Argonne National Laboratory
9700 South Cass Avenue, Argonne, IL 60439, USA
Prof. S. A. Rogers
Department of Chemical and Biomolecular Engineering
University of Illinois at Urbana-Champaign
600 S. Matthews Avenue, Urbana, IL 61801, USA
E-mail: sarogers@illinois.edu

DOI: 10.1002/admi.201701579

fibril composite inks, which have recently been shown to enable theory-directed designs for programmable biomimetic actuators whose environmentally responsive morphological transformations resemble the complex hydronastic dynamics of plants. In practice, optimized NIPAM/Lap materials function poorly as inks for printing structures with microscale design rules, a limitation that follows from the tendency of large-scale aggregates to form within the composite that block flow through small nozzle print heads. Feature dimensions tend to directly impact the performance of devices incorporating these materials, however, in consequence of their sensitivity to transport/diffusion-based kinetics.[1a] Improved ink chemistries for 3D printing, ones that can accommodate designs embedding challenging critical feature sizes as one means to circumvent diffusion-based actuation limits in such devices, is the subject addressed in the current report.

Lap ($Na_{0.7}[(Si_8Mg_{5.5}Li_{0.3})O_{20}(OH)_4]$), a synthetic smectite clay, forms a soft elastic gel when hydrated due to the separation of the individual discs that results in consequence of the associated osmotic force.[12] The addition of polar components (small molecules, organic monomers/polymers, etc.) can elicit changes in the microstructure of the material, from exfoliated particles to larger, more open aggregates (where it is believed that the positive edges of the clay particles variously associate with the negative charges present on the disc faces).[13] Such aggregations of Lap, and in general nanoparticles used to viscosify inks, complicate 3D fabrication by DIW since the aggregates make reliable, microfilament extrusion for high resolution (fine feature width) printing extremely difficult.[14] The current literature reports a limiting feature dimension of 150 µm nozzle for the extrusion of an NIPAM/Lap ink.[1a]

The current work describes an approach to improve the flow properties of composite inks by modifying the aggregation dynamics in ways supporting microfilament extrusion. A model NIPAM/Lap ink system that can be extruded using a 100 µm nozzle, a 33% smaller feature dimension than previously demonstrated, is presented in this work (**Figure 1**a,b). While the NIPAM/Lap ink can be extruded at this reduced nozzle diameter, the production of filaments at this dimension requires high driving pressures and remains severely impacted by significant jamming/tip clogging. We report and characterize here a specific surface modification of a model NIPAM/Lap ink that affords significant improvements both in the reduction of nozzle clogging and a 1.7 reduction of pressure required for microextrusion of filaments over a range of nozzle sizes (330–100 µm, Figure 1c). Most notably, this surface modification does not compromise the resolution of the filaments realized (Figure 1a,b) in 3D fabrication via microscale DIW. While increasing the printing pressure beyond the values examined in Figure 1c remains a means to extrude inks that are prone to clogging at small nozzle diameters, it is not an optimal solution. This reflects the fact that at feature dimensions less than 30 µm, glass capillaries (with lower mechanical allowances for safe printing pressures) are generally substituted for stainless steel nozzles in DIW. For this reason, rheological properties increasingly weigh on the design of suitable ink chemistries.

The data show that the addition of a rheological modifier, sodium pyrophosphate (NaPyrPh), acts to tailor the electrostatic

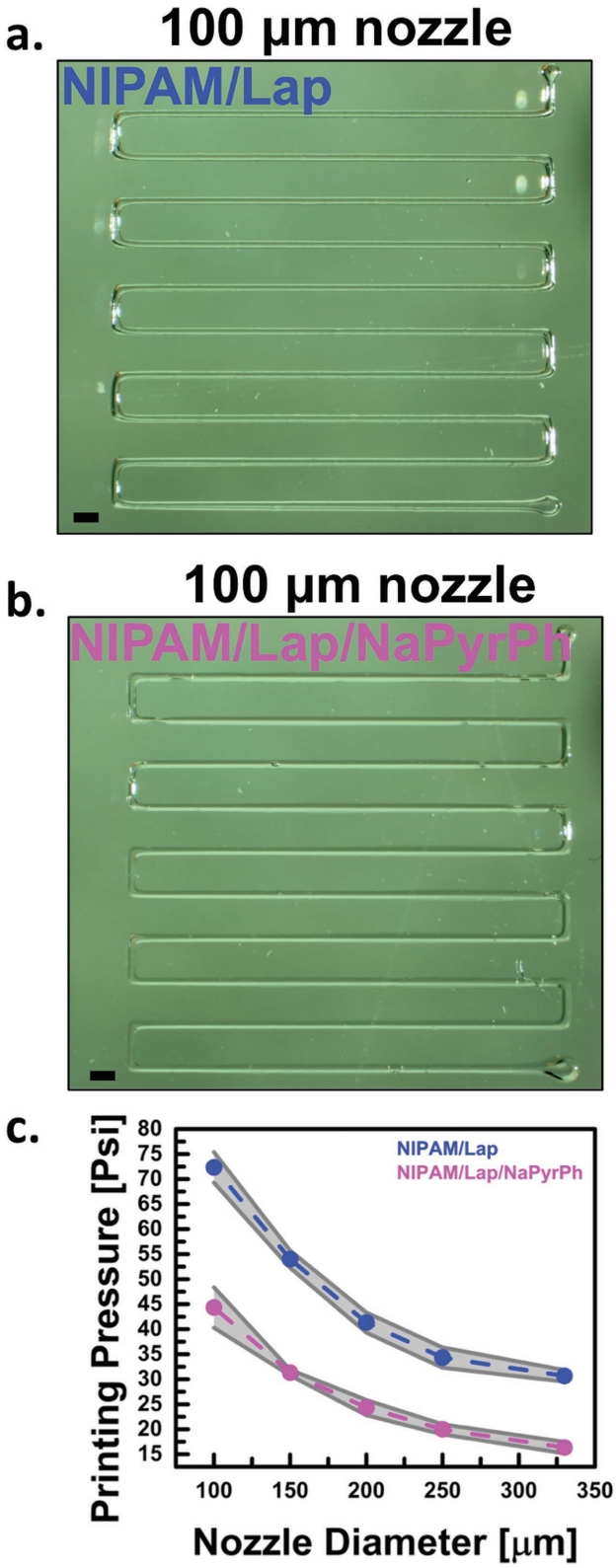

Figure 1. a) DIW NIPAM/Lap ink using a 100 µm nozzle, scale bar 500 µm; b) DIW NIPAM/Lap/NaPyrPh ink using a 100 µm nozzle, scale bar 500 µm; c) minimum printing pressure required for extrusion of composite ink as a function of nozzle diameter with flow rate of 1 mm s^{-1}.

interactions of the Lap platelets, impacting dynamical aspects of the ink's response to shear. Four critical rheological parameters, complex modulus, flow behavior, thixotropy, and yield stress, are evaluated to provide insights into the structure–property relationships that underpin this electrostatic modification of Lap nano-/microstructure within the material to allow significantly improved and finer-scale microfilament extrusion for DIW.

Net form printing requires an ink that can retain its shape when extruded to create a self-supporting 3D structure. To meet this requirement, the composite ink must have a static yield stress and a relatively large modulus below the yield stress. These features can be evaluated by examining a critical rheological parameter, the complex modulus, in the linear regime. The real and imaginary components of the complex modulus, which is the ratio of the complex stress to the complex strain, provide a first-order evaluation of whether or not the ink behaves as a solid in its rest state. The frequency dependence of the magnitude of the complex modulus of the material is examined in the linear viscoelastic region, where deformations and stresses are small enough to probe, but not disturb, the quiescent microstructure. Stress-controlled rheology is employed to closely resemble the pressure-driven printing process. The amplitude of the stress is kept in the linear viscoelastic regime, as determined from amplitude sweeps, while the angular frequency is swept over a wide range. If the magnitude of the complex modulus remains independent of angular frequency, then there is no rate dependence of the material response, and the material is considered to be solid-like with the rheology in this small stress and strain limit dominated by particle–particle interactions. If the magnitude of the complex modulus increases with angular frequency, then there is a clear dependence on the shear rate, and the material is said to exhibit viscoelasticity with a nonzero fluid component. Solid-like behavior is required for printing in order to retain the shape of a filament. A large viscous contribution to the complex modulus would necessarily lead to significant rheological creep, which would manifest as sag of the printed filament. The magnitude of the complex modulus is a good measure to investigate because it provides a clear mechanism for comparison of the stiffness of various materials and provides insight into particle–particle interactions.[15]

The composite ink, NIPAM/Lap, and the composite ink with sodium pyrophosphate (NIPAM/Lap/NaPyrPh) incorporated as an additive (compositions for exemplary inks are given in the Experimental Section) both exhibit solid-like behavior in the linear regime, with the addition of NaPyrPh reducing the magnitude of the complex modulus by approximately a factor of two (**Figure 2**a). Given that the complex modulus has two components, it is also informative to investigate the phase angle difference. The phase angle difference measures the phase lag between the stress and the strain. A small value of the phase angle, which ranges between zero and $\frac{\pi}{2}$, is indicative of

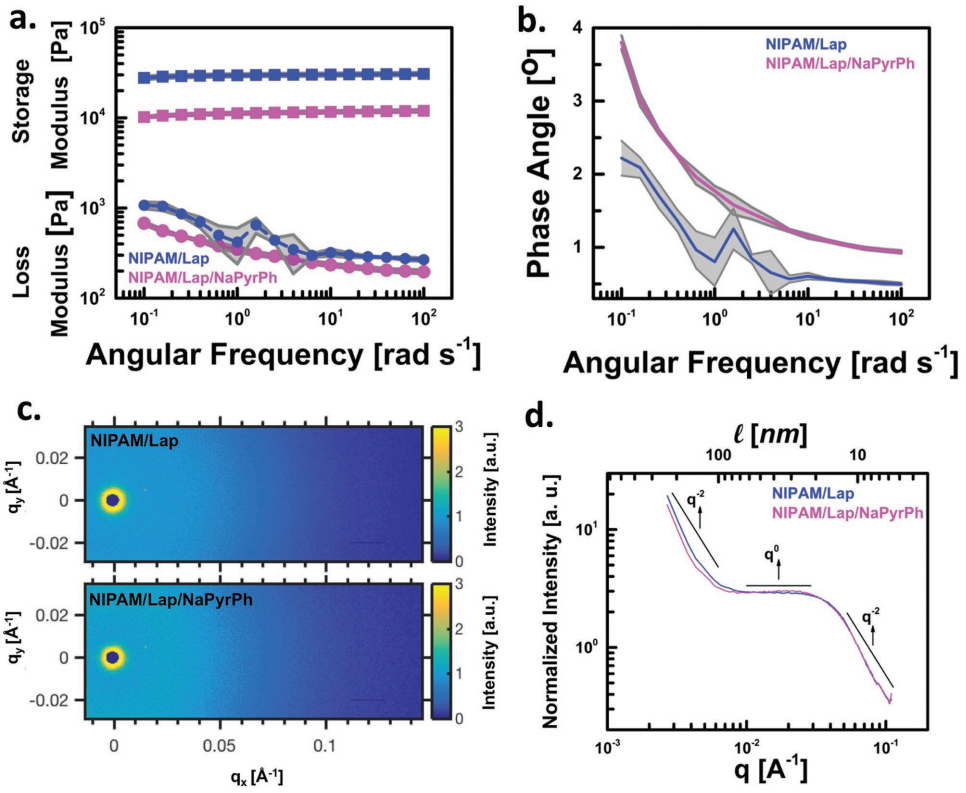

Figure 2. a) Log–log plot of storage (square/solid line) and loss (circle/dash line) modulus as a function of angular frequency measured in oscillatory mode at 50 Pa, error bars are from repeat measurements; b) plot of phase angle as a function of angular frequency measured in oscillatory mode at 50 Pa, error bars are from repeat measurements; c) isotropic 2D scattering patterns after a 10 min preshear (5 s^{-1}); d) log–log plot of 1D scattering curves with intensity normalized.

solid-like behavior. The phase angle difference is also measured to determine the relative contributions of the viscous and elastic components to the complex modulus of the material. Since both inks are gels, the phase angle is relatively small (Figure 2b) indicating the gels are primarily elastic (solid) with strong particle–particle interactions.

Since there is a clear difference in the linear rheology of the two materials, as determined by the complex modulus, small angle X-ray scattering (SAXS) was carried out during the rheological experiments to determine how modifying particle–particle interactions with NaPyrPh alters the microstructure under flow. The 2D scattering patterns for both inks indicate isotropic scattering with no preferential orientation of the Lap particles within the probed length scale(s) (Figure 2c). The 2D scattering patterns are therefore reduced to 1D plots, $I(q)$ versus q by azimuthal averaging, without loss of generality.[16] The 1D plots for both composites (Figure 2d) indicate large-scale, open aggregation of Lap particles with an interparticle spacing, l, of ≈21–83 nm based on the relationship of $l = \frac{2\pi}{q}$.[17] The addition of NaPyrPh results in a softer gel, as evidenced by the lower value of the magnitude of the complex modulus, even as the physical spacing of the microstructure (as measured by SAXS) remains unchanged on the observed length scales. The ability to modify electrostatic interactions to reduce the modulus of the material while maintaining a gel state is a crucial contributor to the printing enhancement evidenced by the drastic reduction in pneumatic pressure required for DIW of the modified composite ink without sacrificing resolution of microfilament (Figure 1).

The second critical rheological parameter to understand is how Lap aggregates in the ink respond to shear during printing. As noted above, both inks exist as gels at small stresses and strains and do not exhibit critical shear rate property dependences under flow (Figure S1, Supporting Information) as also observed in other elastic-dominated printing systems.[18] Since slip is a possibility in the rheological measurements and DIW of the inks, two geometries (stainless steel cone-plate and polycarbonate cup and bob geometries) are used with only minimal differences in the flow behavior (**Figure 3**a). At the highest shear rate, the shear stress falls off for the cone and plate geometry due to sample ejection (which does not occur with the cup and bob geometries). The microstructure was examined using rheo-SAXS in the flow-vorticity plane (1,3) (Figure 3b) before, during, and after applied shear (shear rates of 0, 0.1, 1, 10, and 1000 s^{-1}) (Figure 3c,e). The scattering patterns remained isotropic with increasing shear rate (Figures S2 and S3, Supporting Information). As the applied gap-averaged shear rate increases, there is minimal change noted in the scattering pattern at high q and a slight increase in intensity at low q (Figure 3d,f). At low but nonzero shear rates (0.1 and 1 s^{-1}), we see a small decrease in scattering intensity across all length scales probed for NIPAM/Lap, indicating the number of clusters in the size range probed is reduced by shear. This could be interpreted as evidence of shear-induced structuring, whereby smaller clusters are brought together by low shear rates to form structures that are larger than we can observe. By contrast, in the NIPAM/Lap/NaPyrPh at these low shear rates, the scattering intensity increases for the probed region, indicating that there are more scatterers at these length scales. This increase in population of smaller scatterers can only result from the breakdown of larger structures. While the surface modification appears to affect how the structure of the gel is broken down by shear, we show in Table S1 in the Supporting Information (via two-way ANOVA analysis) that there is no statistical difference in the average SAXS intensity in the entire q range of NIPAM/Lap and NIPAM/Lap/NaPyrPh at all the shear rates tested. There is, however, a statistically significant difference between shear rates for both inks at length scales above 25 nm, as indicated by the low q scattering. The shear rate has a fundamental effect on the number of scatterers that scatter at the length scales probed, suggesting that a microstructural change is responsible for this change in behavior. The microstructure of this material likely includes larger structures, the sizes of which extend beyond the limits probed by the SAXS setup employed (233 nm). As the material is sheared, the large aggregated structures begin to break, which results in the formation of smaller structures that scatter within the experimental window. This is supported by the change in slope in the mid q range (0.00755–0.0301 A^{-1}), where the slope of q decreases from ≈0 to –0.2 (Figure S4, Supporting Information) indicating a loss of structure in the aggregates.[17]

After the material is sheared, the time required for a material to return to its initial state must be very short in order to sustain shape retention by the filaments. Given that the results of the rheo-SAXS experiments indicate that shearing acts to breakdown structure, and that the structures reform once shearing is ceased, we identify these materials as being thixotropic. To investigate the restructuring process, the microstructure of the material is probed via SAXS immediately after the highest shear rate has been removed (Figure 3c–f). For both materials, there is a decrease in the intensity seen at all length scales, with a pronounced decrease at the smallest length scales, which corresponds to recovery of the largest microstructures. Recovery of microstructure is also confirmed by the return of the slope of q to near 0 in the mid q range (Figure S4, Supporting Information).[17] Based on diffusion-limited kinetic aggregation, the smallest structures will recover first with the larger microstructures recovering as time progresses to return to the static structure state (Figure 3g). The variation of the recovery time to the static with the length scale of the microstructure state is an expected dependency for material systems of this type.[19] Despite the long recovery time associated with the reforming of larger scale structures, the prompt recovery seen at small length scales following shear provides the electrostatically modified NIPAM/Lap with a critical capacity to improve print performance, a result of changes in modulus that all the same maintains the rheology of a gel that is comparable in both its flow and thixotropy to an unmodified NIPAM/Lap ink.

The final critical component of the rheology we examined in order to better understand how the strength of the composite material impacts its extrusion as an ink through a nozzle was the yield stress.[20] To do so, a syringe connected to a compressed air pressure controller and fitted with stainless steel nozzles of varying diameters (**Figure 4**a; Figure S5, Supporting Information) was used to conduct rheocapillary extrusion experiments. The 2D scattering patterns of NIPAM/Lap and NIPAM/Lap/NaPyrPh

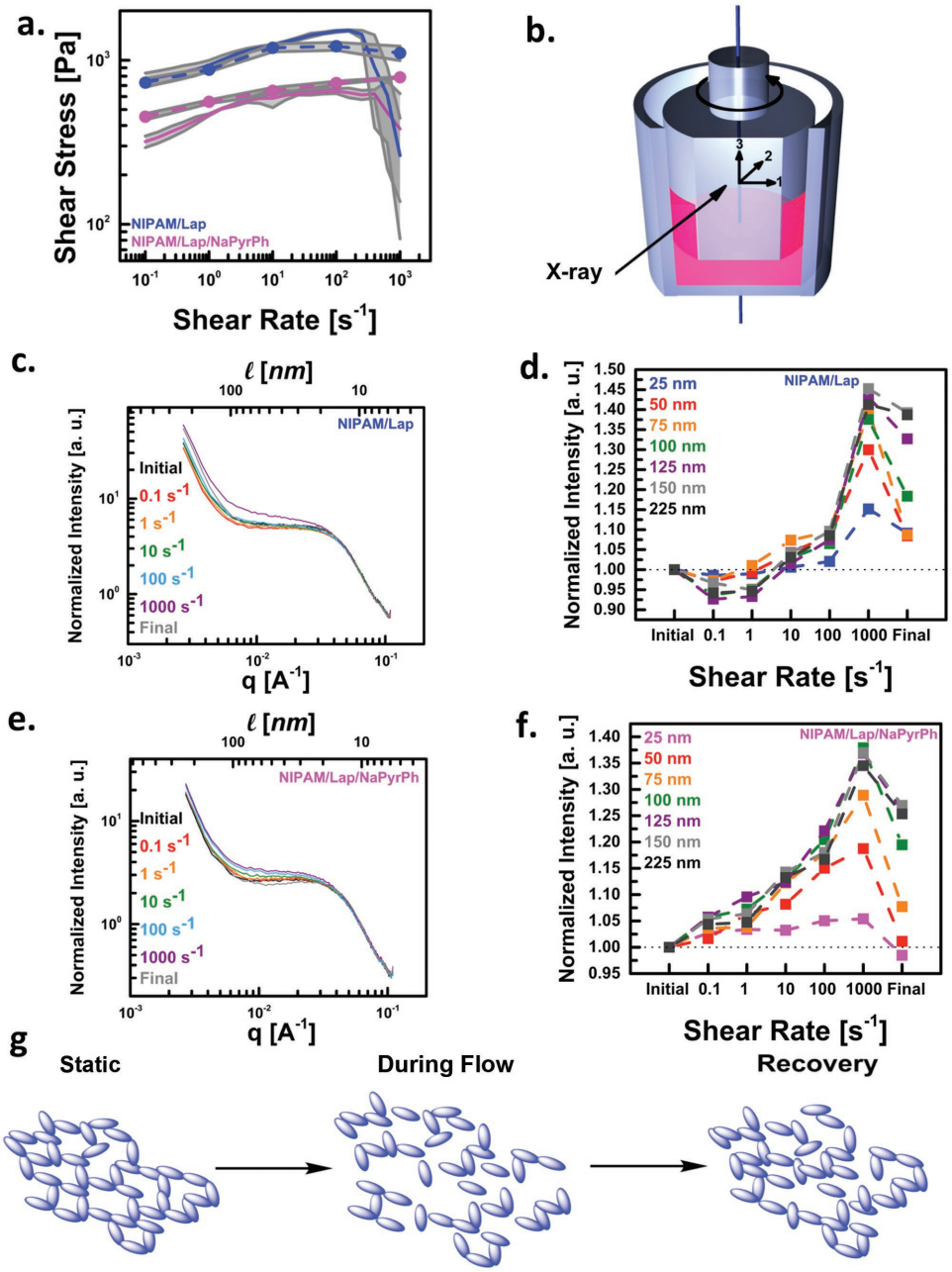

Figure 3. a) Log–log plot of shear stress as a function of shear rate (circle—cup and bob, line— cone and plate), error bars are from repeat measurements; b) SAXS with in situ shear setup to probe 1,3 plane; c) log–log plot of 1D scattering curves of NIPAM/Lap of intensity as a function of shear rate (0.1, 1, 10, 100, and 1000 s^{-1}, final (shear stopped, 0 s^{-1})) with intensity normalized to initial (0 s^{-1}); d) average intensity changes in scattering curves of NIPAM/Lap normalized to initial (0 s^{-1}) as a function of shear rate at different length scales; e) log–log plot of intensity of 1D scattering curves of NIPAM/Lap/NaPyrPh of intensity as a function of shear rate (0.1, 1, 10, 100, 1000 s^{-1}, final (shear stopped, 0 s^{-1})) with intensity normalized to initial (0 s^{-1}); f) average intensity changes in scattering curves of NIPAM/Lap/NaPyrPh normalized to initial (0 s^{-1}) as a function of shear rate at different length scales; g) microstructure of Lap in composite inks at static time, during flow, and recovery.

extruded from a 100 µm diameter tip are compared as an exemplary case (Figure 4b, note that now q_y is the flow direction). The NIPAM/Lap/NaPyrPh filament is anisotropic as evidenced by two broad peaks at $q\_y = 0.03$ A^{-1}. In contrast, the NIPAM/Lap filament has less anisotropy. The difference in the anisotropy of the two filaments is due the presence of NaPyrPh, which assists in the reconfiguration of Lap platelets during confinement and extrusion through a nozzle. The reconfiguration facilitates flow through the nozzle as evidenced by the difference in required pressure for extrusion (Figure 1c) and is consistent with the decrease in modulus and yield stress of the NIPAM/Lap/NaPyrPh sample. A quantitative analysis of the yield stress is necessary in order to fully understand the difference that exists in consequence of shearing the material through a nozzle.

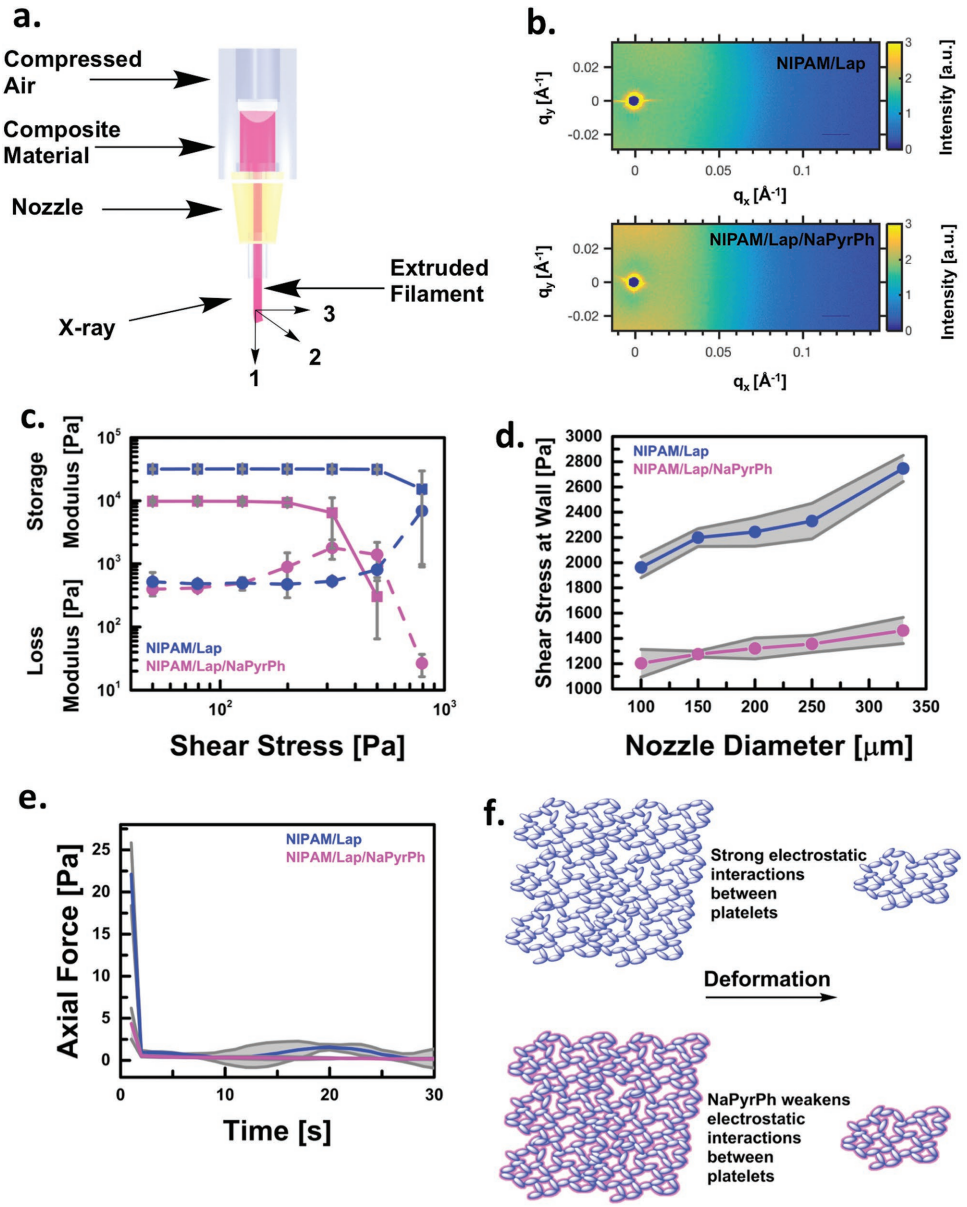

Figure 4. a) Pneumatic extrusion of ink through a nozzle; b) 2D scattering patterns of composite inks at 0.3 mm below 100 μm nozzle during extrusion; c) log–log plot of storage (square/solid line) and loss (circle/dash line) modulus as a function of shear stress measured in oscillatory mode at 1 rad s^{-1}, error bars are from repeat measurements; d) shear stress of composite ink at wall as a function of nozzle diameter with flow rate of 1 mm s^{-1}, error bars are from repeat measurements; e) axial force as a function of time during preshear (5 s^{-1}) measured immediately after loading sample, error bars are from repeat measurements; f) dominant intermolecular interactions disrupted due to deformation of composite ink during extrusion.

The complex moduli of the composite inks were measured with a 109.5 μm gap to determine how much pressure must be applied to the material before it flows. The minimum stress to induce flow, or yield stress, is defined as the stress at G′–G″ crossover (Figure 4c), and those for NIPAM/Lap and NIPAM/Lap/NaPyrPh are 1000 and 300 Pa, respectively. The yield stress measured in the bulk rheology can be compared with the apparent shear stress applied at the wall of the nozzle (τ_y) during extrusion of filament as calculated by Equation (1)

$$\tau_\gamma = \frac{(P_{\text{flow}} - P_{\text{atm}})r}{2L} \quad (1)$$

where P_{flow} is the minimum pressure required to extrude the filament at 1 mm s^{-1}, P_{atm} is the atmospheric pressure, r is the radius of the nozzle, and L is the length of the nozzle.[18] For all nozzle diameters, the apparent shear stress applied at the wall for NIPAM/Lap/NaPyrPh is lower than NIPAM/Lap as expected. For both compositions, the apparent shear stress applied at the wall of a 100 μm nozzle ($\tau_{y\,\text{app}}$) during extrusion was greater than

their respective yield stresses as deduced in the bulk rheology measurements with a comparable gap size (Figure 4d). This difference in the apparent shear stress may be due to 1D confinement (velocity gradient) in bulk rheology measurements is not enough to enforce the structure from 2D confinement (velocity gradient and vorticity) that leads to the higher yield stress during 3D printing. For example, in the bulk rheology experiments, we tested different gap heights, but the material is still able to freely reorganize its structure in the two directions parallel to the plates, whereas, in the printer application, the only free axis is in the flow direction. With this caveat, the data, when taken together, suggest a critical role that surface chemistry might play in order to account for why the shear stresses seen at the wall are significantly higher than the yield stresses of the materials themselves.

We infer that the added NaPyrPh polyanion likely preferentially adsorbs onto/associates with the positively charged edges of the Lap platelets, giving the whole particle an overall large negative charge. This provides a schematic mechanism through which the energetics of platelets sliding past each other are modified, one based on varying magnitudes of particle–particle electrostatic repulsions (and correlated bridging interparticle interactions), during shearing to allow for reconfiguration of Lap. The latter inference is in fact one that is confirmed by independent particle zeta (ζ) potential measurements, which showed values that were more negative in the composite with NaPyrPh, a result indicative of adsorbed pyrophosphate ($P_2O_7^{4-}$) on the Lap edges (Figure S6, Supporting Information). This surface chemistry modification is crucial for printing since the material is in a relaxed state in the syringe reservoir, but does not have time or mechanism to return to a relaxed state as it comes through a constricted geometry and is extruded. One notes that, when the materials are confined in the cone and plate geometry, an axial force is measured during the preshear treatment as a low shear rate is applied to relax and remove residual normal stress to negate sample loading effects; this axial force decreases as the material is sheared (Figure 4e). The axial force seen here is a measurement of how the sample exerts force against its container and relates to the axial force the sample exerts when extruded through a constricted geometry. While both materials exert an axial force when initially confined in the sample cell, the axial force of NIPAM/Lap is four times greater than NIPAM/Lap/NaPyrPh. This strongly suggests that the NIPAM/Lap system is more resistant to flow and reorganization of Lap platelets due to stronger (less screened) interparticle interactions between the platelets (Figure 4f), which also results in the elevated magnitude of the shear stress seen at the wall during printing.

Four critical rheological properties—complex modulus, flow, thixotropy, and yield stress—allow the design of an improved NIPAM/Lap ink for DIW based on an electrostatic modification of polymer/clay interactions. Selective modification of the surface charge of the Lap allows a useful reduction in the complex modulus and yield stress, while maintaining comparable flow behavior and thixotropy of their composite NIPAM gels. The retention of the large, open aggregation of the Lap, but with charge screening provides the necessary customization to these composite materials to provide a mechanism to shear platelets and improve printability without disrupting the microstructure necessary to retain a gel state for building structures. We exploit this printing-centric approach experimentally in the ability to extrude the electrostatically modified composite using a 100 µm nozzle, which represents a 33% reduction (i.e., smaller) nozzle diameter than the current literature reports for Lap[1a] and particle-based inks.[21] The mechanistic insights gained through improved understandings of the impacts of surface modification of Lap in a model particle-stabilized yield-stress fluid ink for DIW provide a general guideline to inform materials design—one demonstrating principles that can be used to tailor rheological properties, while maintaining a yield-stress fluid with a high thixotropy to allow printing of small filaments with high aspect ratios, reduced failures due to particle aggregation, while allowing reductions in the required extrusion pressures. The diameter of the extruded filament documented in the sections above is not in this sense then a limiting case. Using the explicit impacts of this surface modification as a guide, smaller feature dimensions of polymer/clay composites should be achievable due to the ability to use glass capillaries in consequence of the lower pressures required for extrusion. Our own work going forward will seek to use this mechanistic insight for surface modification of composite inks to improve mass-transfer characteristics in soft devices—notably chemo-mechanical actuators—and tissue engineering by exploiting materials of this class.

Experimental Section

Composite Ink Preparation: Irgacure 2959 (Sigma-Aldrich, 0.015 g), sodium pyrophosphate decahydrate (Sigma-Aldrich, 0.015 g), NIPAM (Sigma-Aldrich, unmodified, 0.30 g), Lap XLG clay (BYK Additives, unmodified, 0.360 g), and Milli-Q water (2.34 mL) were hand mixed and then mixed using a Thinky Mixer (ARE-310, Thinky) in a closed container. The gel was stored in the dark for 24 h before characterization.

Rheological Characterization: Inks were characterized using a rheometer (DHR-3, TA instruments) in a cone-plate geometry (40 mm diameter, 4.005°, 109.5 µm gap height) at 25 °C. A preshear of 5 s^{-1} for 10 min followed by 1.0×10^{-4} s^{-1} for 10 min was applied after sample loading. Oscillation amplitude experiments were conducted with a constant angular frequency (1 rad s^{-1}) using a logarithmic stress sweep (50.0–1000.0 Pa). Oscillation frequency experiments were conducted with a constant stress (50.0 Pa) with a logarithmic angular frequency sweep (0.1–100.0 rad s^{-1}). Flow experiments were conducted with a logarithmic shear rate sweep (0.1–1000.0 s^{-1}). All experiments were repeated three times to obtain error bars.

Capillary Extrusion Characterization: Ink was loaded into a Luer-lock syringe, mounted to a 3D printer with camera, and attached to a compressed air regulator (Ultimus V Pressure Controller, Nordson EFD). Stainless steel, straight tip nozzles (100–330 µm, 10 mm nozzle length, Nordson EFD) were attached to the syringe via a Luer-lock connection. For each tip diameter, 5 psi was applied to the system for 10 s. If no ink extruded, the pressure was increased in increments of 5 psi until the pressure was sufficient for the material to be extruded at a linear flow rate of 1 mm s^{-1}. All experiments were repeated three times to obtain error bars. The print path (G-code) is available upon request.

Rheo-SAXS: Measurements were conducted at beam line 8-ID-I of the Advanced Photon Source Argonne National Laboratory, Lemont, IL using 7.34 keV X-rays. A direct-illuminated charge-coupled device (CCD) area detector (Pilatus 100K, pixel size of 172 µm, 487 × 195 pixels) that was 3930 mm from the sample was used to measure scattering intensity from $0.003\ A^{-1} < q < 0.11\ A^{-1}$ in the vorticity direction. Using the magnitude of q, the pixels were partitioned for analysis. For bulk rheology, inks were characterized with a rheometer (MCR 301, Anton-Paar instruments) with a custom-made cylindrical Couette Cell with a 500 µm gap at 30 °C in the 1,3 (flow-vorticity) plane. A preshear of 5 s^{-1} for 10 min was applied before each

flow experiment. It was determined that this gave reproducible results in the linear viscoelastic regime across multiple loadings and sample preparations. A scattering pattern was measured before and after the flow experiments. Flow experiments were conducted with a logarithmic shear rate sweep (0.1–1000.0 s^{-1}). The shear rate was held constant for 60 s prior to collection of each scattering pattern with a minimum of 18 scattering patterns averaged per shear rate. For capillary extrusion experiments, the setup as described previously was used and the syringe was mounted such that the tip of the nozzle was 0.3 mm above the path of the beam. The material was continuously extruded, and scattering patterns were collected (50 averaged per nozzle). All experiments were repeated three times to obtain error bars.

Imaging: A stereoscope (Olympus, SZX7) was used to image 3D direct-ink written samples.

Supporting Information

Supporting Information is available from the Wiley Online Library or from the author.

Acknowledgements

The authors gratefully acknowledge funding from the Army Research Office (W911NF-13-0489). Experiments were carried out in part in the Frederick Seitz Materials Research Laboratory Central Research Facilities, University of Illinois at Urbana-Champaign. Use of the Center for Nanoscale Materials and the Advanced Photon Source, Office of Science User Facilities, was supported by the U.S. Department of Energy, Office of Science, Office of Basic Energy Sciences, under Contract No. DE-AC02-06CH11357.

Conflict of Interest

The authors declare no conflict of interest.

Keywords

direct-ink write, hydrogels, nanocomposites, polymers, rheo-SAXS

Received: December 2, 2017
Revised: December 31, 2017
Published online: February 12, 2018

[1] a) A. S. Gladman, E. A. Matsumoto, R. G. Nuzzo, L. Mahadevan, J. A. Lewis, *Nat. Mater.* **2016**, *15*, 413; b) B. Chen, S. Liu, J. R. G. Evans, *J. Appl. Polym. Sci.* **2008**, *109*, 1480.
[2] a) V. I. Paz Zanini, M. Gavilan, B. A. Lopez de Mishima, D. M. Martino, C. D. Borsarelli, *Talanta* **2016**, *150*, 646; b) P. W. Faguy, W. Ma, J. A. Lowe, W.-P. Pan, T. Brown, *J. Mater. Chem.* **1994**, *4*, 771.
[3] a) M. Shen, L. Li, Y. Sun, J. Xu, X. Guo, R. K. Prud'homme, *Langmuir* **2014**, *30*, 1636; b) P.-I. Au, S. Hassan, J. Liu, Y.-K. Leong, *Chem. Eng. Res. Des.* **2015**, *101*, 65; c) P. Mongondry, T. Nicolai, J. F. Tassin, *J. Colloid Interface Sci.* **2004**, *275*, 191.
[4] J. M. McCracken, A. Badea, M. E. Kandel, A. S. Gladman, D. J. Wetzel, G. Popescu, J. A. Lewis, R. G. Nuzzo, *Adv. Healthcare Mater.* **2016**, *5*, 990.
[5] Z. Wu, X. Su, Y. Xu, B. Kong, W. Sun, S. Mi, *Sci. Rep.* **2016**, *6*, 24474.
[6] S. Hong, D. Sycks, H. F. Chan, S. Lin, G. P. Lopez, F. Guilak, K. W. Leong, X. Zhao, *Adv. Mater.* **2015**, *27*, 4035.
[7] a) C. Yu, Z. Duan, P. Yuan, Y. Li, Y. Su, X. Zhang, Y. Pan, L. L. Dai, R. G. Nuzzo, Y. Huang, H. Jiang, J. A. Rogers, *Adv. Mater.* **2013**, *25*, 1541; b) P. Yuan, O. Kuksenok, D. E. Gross, A. C. Balazs, J. S. Moore, R. G. Nuzzo, *Soft Matter* **2013**, *9*, 1231.
[8] Liang, J. Liu , X. Gong, *Langmuir* **2000**, *16*, 9895.
[9] S. K. Mujumdar, R. A. Siegel, *J. Polym. Sci., Part A: Polym. Chem.* **2008**, *46*, 6630.
[10] S. Liu, G. Gao, Y. Xiao, J. Fu, *J. Mater. Chem. B* **2016**, *4*, 3239.
[11] Y. Ye, Q. Wang, *RSC Adv.* **2015**, *5*, 7752.
[12] B. Ruzicka, E. Zaccarelli, *Soft Matter* **2011**, *7*, 1268.
[13] S. Jatav, Y. M. Joshi, *Appl. Clay Sci.* **2014**, *97*, 72.
[14] C. Minas, D. Carnelli, E. Tervoort, A. R. Studart, *Adv. Mater.* **2016**, *28*, 9993.
[15] D. Therriault, S. White, J. Lewis, *Appl. Rheol.* **2007**, *17*, 1.
[16] Z. Jiang, *J. Appl. Crystallogr.* **2015**, *48*, 917.
[17] E. Loizou, P. Butler, L. Porcar, E. Kesselman, Y. Talmon, A. Dundigalla, G. Schmidt, *Macromolecules* **2005**, *38*, 2047.
[18] J. Bruneaux, D. Therriault, M.-C. Heuzey, *J. Micromech. Microeng.* **2008**, *18*, 115020.
[19] N. Willenbacher, *J. Colloid Interface Sci.* **1996**, *182*, 501.
[20] K. Cai, J. Sun, Q. Li, R. Wang, B. Li, J. Zhou, *Appl. Phys. A* **2010**, *102*, 501.
[21] J. T. Muth, P. G. Dixon, L. Woish, L. J. Gibson, J. A. Lewis, *Proc. Natl. Acad. Sci. USA* **2017**, *114*, 1832.